Internal insulation of solid masonry walls - Field experiment with Phenolic foam and lime-cork based insulating plaster

Jensen, Nickolaj Feldt; Rode, Carsten; Andersen, Birgitte; Bjarløv, Søren Peter; Møller, Eva B.

Published in:
E3S Web of Conferences

Link to article, DOI:
10.1051/e3sconf/202017201003

Publication date:
2020

Document Version
Publisher's PDF, also known as Version of record

Internal insulation of solid masonry walls – field experiment with Phenolic foam and lime-cork based insulating plaster

Nickolaj Feldt Jensen[1,*], *Carsten* Rode[1], *Birgitte* Andersen[2], *Søren Peter* Bjarløv[1], and *Eva B.* Møller[1]

[1]Department of Civil Engineering, Technical University of Denmark, Brovej 118, 2800 Kgs. Lyngby, Denmark
[2]Department of Biotechnology and Biomedicine, Technical University of Denmark, Søltofts Plads Building 221, 2800 Kgs. Lyngby, Denmark

Abstract. The study investigated the hygrothermal performance and risk of mould growth in two thermal insulation systems for internal retrofitting purposes; a phenolic foam system with a closed cell structure, and a capillary active diffusion-open lime-cork based insulating plaster. The setup consisted of a 40-feet (12.2 m) insulated reefer container with controlled indoor climate, reconfigured with several holes (1x2 m each) containing solid masonry walls with embedded wooden elements on the interior side and different interior insulation systems, with and without exterior hydrophobisation. Focus was on the conditions in the interface between wall and insulation system, and in the embedded wooden elements. Relative humidity and temperature were measured in several locations in the test walls over two years, and the mould risk was evaluated by measurements and the VTT mould growth model. Findings for the interior phenolic foam system indicated that exposed walls experienced high relative humidity and high risk of moisture-induced problems. Exterior hydrophobisation had a positive effect on the moisture balance for the southwest oriented wall with phenolic foam. The lime-cork based insulating plaster showed high relative humidity and risk of moisture-induced problems, with and without hydrophobisation.

1 Introduction

A high energy saving potential is found in retrofitting of historic masonry external walls [1]. Solid masonry buildings from 1850-1930 account for 41% of all Danish multi-story residential buildings (3-6+ floors) [2]. Studies have shown average-weighted U-values of 0.83 and 1.12 W/m2·K for external walls in multi-story residential buildings built prior to 1850 and the period 1850-1930, respectively [1]. Many of these buildings are worthy of preservation, which often prohibits major exterior alterations. From a building physics point of view, internal post-insulation of solid masonry walls is considered problematic as the reduced heat flow to the existing wall results in a lower temperature gradient and the original wall becomes colder [3], [4]. This increases the risk of interstitial condensation [3], [4]. Moreover, inwards drying is also reduced due to the increased diffusion resistance [3]. The higher moisture levels lead to increased risk of moisture-induced damages [3], [5], [6]. In the past two decades, strategies for internal insulation have changed away from diffusion-tight systems to diffusion-open capillary active systems, capable of redistributing moisture to reduce the mould risk. Studies [7]–[9] have observed good performance using diffusion-open capillary systems for internal retrofitting. However, other studies [5], [10] have found better performance for the diffusion-tight systems if rain could be prevented. Driving rain is one of the largest contributors to moisture in buildings [3] and a crucial factor regarding performance of internally insulated solid exterior walls [5], [10], [11]. Exterior rain protection like hydrophobisation is occasionally proposed for preservation worthy buildings. Insulation manufacturers claim that mould growth is prevented if highly alkaline glue mortars are used for installation of insulation products. This has led to increased focus on alkalinity of the glue mortars. The purpose of this study was to assess the hygrothermal performance of two internal insulation systems in a temperate Nordic climate. The aims were: 1) determine the effect of exterior hydrophobisation on the hygrothermal performance of the examined insulation systems, and 2) test whether mathematical mould models would be useful for prediction of mould risk in the interface and embedded wooden elements.

2 Method and materials

A large experimental setup was constructed by the Department of Civil Engineering at the Technical University of Denmark (DTU) on the test site in Kongens Lyngby, Denmark (55.79°N, 12.53°E). The setup comprised of several test walls constructed to emulate a section of a Danish historic multi-story building from the period 1850-1930, in relation to both design and materials. The setup consisted of a 40-foot insulated reefer container with sixteen 1 x 2 m cut outs made in the façades to accommodate the test walls. Next,

* Corresponding author: nicf@byg.dtu.dk

sixteen identical solid masonry walls with the dimensions (HxWxD) 1987 mm by 948 mm by 358 mm (1½ stones thick with 10 mm interior rendering) were constructed in the cut outs (Fig 1). The test walls were constructed as a 3-dimensional set-up including a wooden interior floor construction and a 108 mm (½-stone) interior separation wall made of masonry with render on both sides. The wooden floor construction consisted of a 175 x 175 mm wooden beam end embedded 100 mm into the masonry wall, supported by a 100 x 100 mm embedded wooden wall plate. The floor construction was closed off using 15 mm oriented strand board (OSB) as flooring, and 100 mm mineral wool emulated the clay-pugging layer, which is traditionally placed between the floor beams. Special care was made to reduce potential sources of error from unintentional heat, air or moisture transport. Measures included: 1) Hygric and thermal decoupling with vapour barrier and mineral wool around each test wall, 2) sealing of exterior joints with mastic sealant, 3) Gutters and flashings against unintentional rain intrusion, and 4) prevention of rain splash-up from the ground.

Nine of the sixteen test walls are presented in this paper, and the wall configurations are presented in Table 1. The applied insulation included: 1) phenolic foam with a closed cell structure, and 2) a capillary active diffusion-open lime-cork based insulating plaster [12]. A wall with a traditional interior insulation system of mineral wool and vapour barrier system was included for comparison. The insulation systems were applied to the "base walls", while two test walls were left as uninsulated reference walls: G3 (Southwest oriented) and G14 (Northeast oriented). Exterior surfaces were kept as bare brick, except for G6, G9, and G11, which were treated with a silane/siloxane-based hydrophobising cream. Prior to the experimental period reported in this paper, which started Dec. 1st 2017, the test walls were fitted with different insulation systems for a period of 2½ years, and the hydrophobisation was applied in connection with the original insulation systems. Insulation systems were dismantled (including the rendering layer on the brick) and the test walls thoroughly cleaned for inorganic residues before application of new render and insulation systems. The mineral wool wall and the reference walls were installed on May 1st 2015. The phenolic foam was installed on November 21st 2017, while the insulating plaster was installed on November 7th 2018.

Temperature and RH were measured and logged every 10 minutes using digital HYT221 sensors in nine different locations in each test wall and in the indoor and outdoor climates. Sensor accuracy was 0.2 K between 0 and 60°C, and 1.8% RH at 23°C between 0 and 90% RH. Sensor range was -40 to 125°C and 1 to 100% RH. Sensors were calibrated prior to installation. The indoor environment was conditioned to 20 °C and 60% relative humidity throughout the whole measuring period (Nov. 2017 to Dec. 2019), no cooling or dehumidification was used, therefore temperature and relative humidity could exceed this level in summer. The indoor moisture load corresponded to the highest humidity class for dwellings (humidity class 3) in Danish context. The moisture load was meant to stress the test walls, without being unrealistically high. Furthermore, two fresh air fans provided an air change rate of approximately 0.5 h^{-1}. The influence of driving rain and high/low solar irradiation was assessed by orienting five of the nine test walls southwest (237°), and four towards northeast (57°).

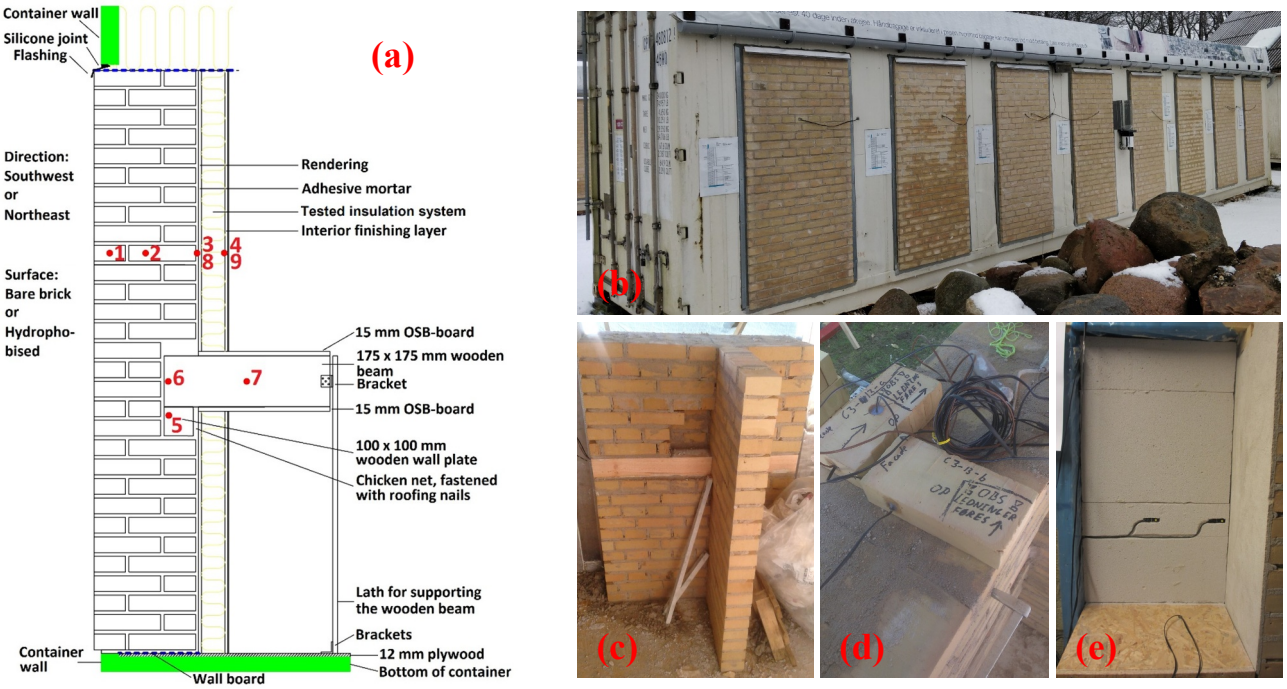

Fig. 1. Test stand configuration: (a) Vertical section of a test wall, (b) External view of test container, (c) Test wall under construction with wooden wall plate and hole for beam end, (d) Sensor installation in bricks (sensor points 1 and 2), (e) Sensor installation in insulation near interior surface (sensor points 4 and 9).

Table 1. Wall configurations and properties used in the field study. Insulation systems were applied internally to the base wall, while two un-insulated base walls were used as reference walls. SW = Southwest, NE = Northeast, +H = with exterior hydrophobisation.

No. of walls: Wall ID & orientation	Material layers (exterior side on top and interior side in the bottom)	Density [kg/m^3]	λ_{dry} [W/(m·K)]	μ_{dry} [-]	A_w [kg/(m^2·s$^{1/2}$)]	d [mm]	R [m^2·K/W]	Z [m^2·s·Pa/kg]
9 Base walls: (serve also as the two reference walls G3 and G14)	Yellow masonry brick*	1643	0.600	16.9	0.278	348	0.58	2.97E+10
	7.7% lime mortar render*	1243	0.440	22.4	0.390	10	0.02	1.13E+09
	Total: existing wall						**0.60**	**3.08E+10**
1 wall: G1_MW_SW	Mineral wool	37	0.040	1	0	100	2.50	5.05E+08
	Vapour barrier			700000		0.2		7.07E+11
	Gypsum board	850	0.177	10	0.277	13	0.07	6.57E+08
	Total: MW system						**2.57**	**7.08E+11**
4 walls: G5_Phenolic_SW G6_Phenolic+H_SW G11_Phenolic+H_NE G12_Phenolic_NE	Adhesive mortar	1516	0.733[1]	41.4	0.006	5	0.01	1.05E+09
	Glass fleece	295	0.200	369	0.405	0.1	0.001	1.86E+08
	Phenolic foam	35	0.020	114	0.009	100	5.00	5.76E+10
	Aluminium foil			10000		0.1		5.05E+09
	Gypsum board	850	0.177	10	0.277	13	0.07	6.57E+08
	Total: Phenolic system						**5.08**	**6.45E+10**
2 walls: G8_Plaster_SW G9_Plaster+H_NE	Insulating plaster	250	0.037	3	0.129	40	1.08	6.06E+08
	Finish render** [2]	1600	0.769	14.6		10	0.01	1.36E-11
	Total: Render system						**1.09**	**1.34E+09**

*materials tested by Technische Universität Dresden within the RIBuild project, unmarked parameters were from the Delphin materials database or manufacturer information. **Natural hydraulic lime NHL 3.5 mortar (35/65/500) with 0-2 mm quartz sand. [1]Estimated value based on 14 mortar products with similar density from the Delphin materials database. [2]Estimated values based on 17 mortar products with similar density from the Delphin materials database.

The widely used VTT mould model by Hukka and Viitanen [13] was used to produce a theoretical prediction of the risk of mould growth. Model output is the mould index (MI), ranging from 0 to 6, where 0 corresponds no growth and 6 to heavy growth (100% coverage). Values 3-6 are within the visual range.

The interface (point 3) was modelled as "medium resistant" with decline factor "relatively low". Embedded wooden elements (point 5 and 6) and points 3 for wall G1 were modelled as "sensitive" with decline factor "wood recession". Mould predictions for the interface were started after one year (on 01-05-2016) to emulate the effect of the alkaline conditions during the initial dry out process for systems using adhesive mortars. Modelling results were compared with the on-site Mycometer results.

Mould growth was analysed using on-site Mycometer [14] surface test in the interface between existing wall and insulation system and Mycometer bulk material test to assess mould growth in different layers through the insulation system (outermost 10 mm, and the remaining thickness was split in two equally sized parts).

Interface samples were taken using sterile cotton buds, while the 80 mm drilling cores were disassembled and prepared in the laboratory for the bulk material test. Mould testing was performed in December 2019, two years after installation of the phenolic foam and one year after the insulating plaster.

The obtained Mycometer values (MV) were evaluated according to protocol: Green (normal background level) = MV ≤ 25 (surface) or MV ≤ 150 (material), Yellow (above normal background level) = 25 < MV < 450 (surface) or 150 < MV < 450 (material), Red (high level of fungi) = MV > 450.

The pH-value of internal lime render and adhesive mortars used for the test walls was determined by mixing 5 g of material powder with 12.5 ml demineralized water, then shaking the samples for 60 minutes at 260-270 rpm. After a 10 min settling period, samples were tested using a Sension+ MM374 (accuracy: ≤0.002 pH). Two tests were performed for each material sample.

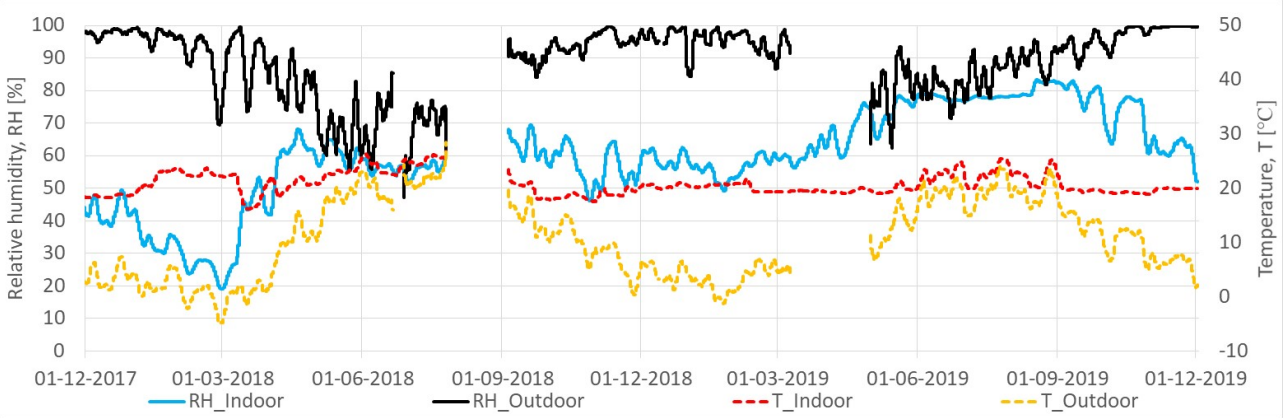

Fig. 2. Relative humidity and temperature for the indoor and outdoor climates

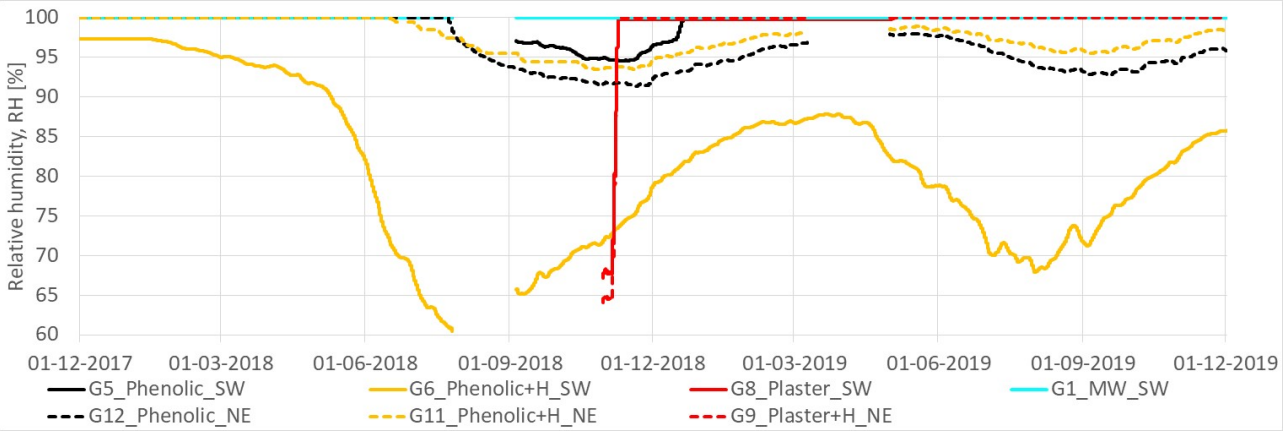

Fig. 3. Measured RH in the interface between wall and insulation systems (measuring point 3). SW: Southwest, NE: Northeast, and +H: wall with exterior hydrophobisation.

3 Results and discussion

Graphical representations of measurement data in the results section are based on 96 hours running average. Hourly data were used for the mathematical mould modelling. Plot abbreviations as presented in Table 1.

3.1. Measurements

The measured indoor and outdoor boundary conditions for the experimental setup is presented in Fig. 2. The drop in indoor RH levels in early 2018 was due to a malfunctioning humidifier. The warm dry summer of 2018 is also visible from Fig. 2, where the indoor RH did not reach as high levels as the more typical Danish summer of 2019.

Measurements for the interface between the masonry wall and insulation systems (Fig. 3) showed that the test walls experienced rather high RH levels throughout the experimental period, except for the hydrophobised wall G6. The internal side of the existing wall structure experienced reduced temperatures after installation of the internal insulation, resulting in the higher RH levels between the wall and insulation system. With the current measurement data, the insulating plaster was seen to perform worse than the phenolic foam insulation. The high RH levels in the interface are likely due to the large amount of water added during installation, increasing moisture levels in the critical locations until the built-in moisture has had sufficient time to dry out. The sensors were still in operation despite showing near 100% RH, and have been seen to perform well in other tests when RH levels start to decrease. To the southwest, both of the assessed insulation systems showed (very high) RH levels similar to the traditional mineral wool system, with only a minor drop for the phenolic foam insulation during the warm dry summer of 2018. The poor performance of the phenolic foam was likely caused by solar-driven vapour flow from the outside towards the inside during periods with shifting rain fall and solar exposure (summer condensation), condensing on the internal side of the masonry wall due to the tight nature of the systems – as described in [3]. Comparison between orientations showed slightly reduced RH levels towards the northeast for the phenolic foam insulation, while the insulating plaster showed similar levels for both cardinal directions. Application of the exterior hydrophobisation had a positive effect on the performance of the southwest oriented wall with phenolic foam, highly reducing the RH levels as rain intrusion was reduced. However, the positive effect was not seen for the northeast oriented wall.

Measurements for the wooden wall plate (Fig. 4) showed increasing RH levels for both the phenolic foam

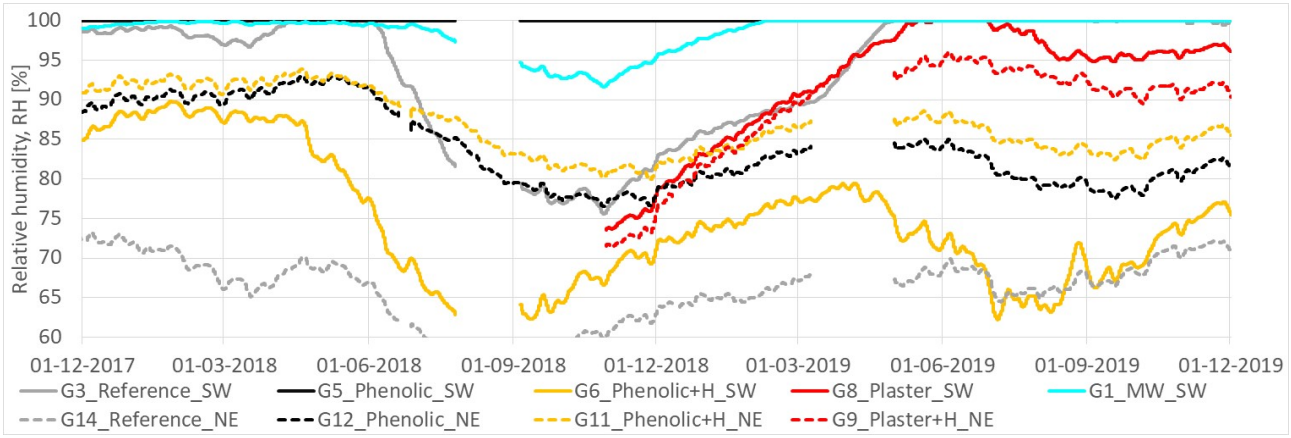

Fig. 4. Measured RH in the wall plate (point 5). SW: Southwest, NE: Northeast, and +H: wall with exterior hydrophobisation.

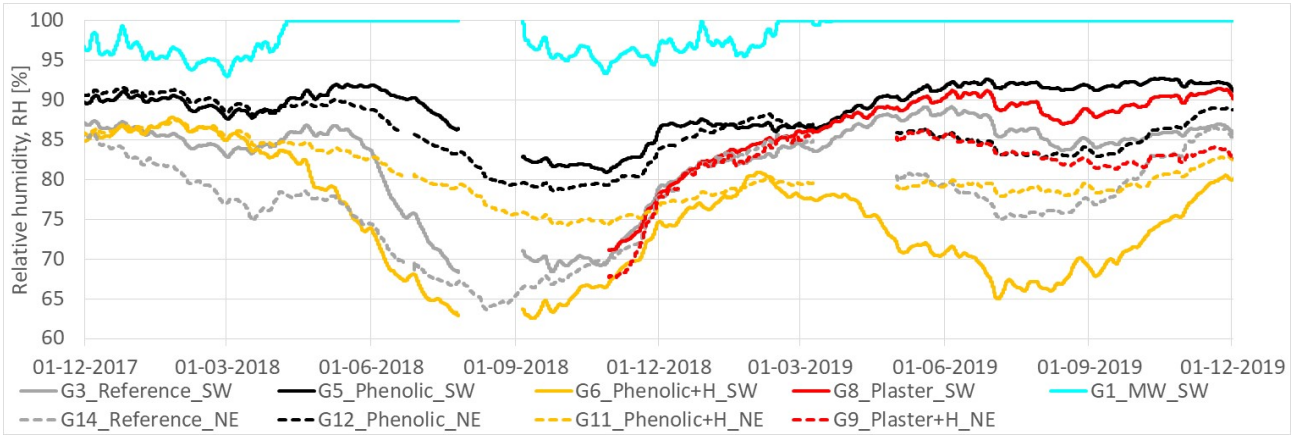

Fig. 5. Measured RH in the beam end (point 6). SW: Southwest, NE: Northeast, and +H: wall with exterior hydrophobisation.

and insulating plaster compared with the reference walls, as the insulation system reduced temperatures in the existing structure and inwards drying. The only exception was the southwest oriented wall with insulating plaster, which showed similar levels.

Comparison between orientations showed that the higher rain load from southwest had a large impact on the performance of the walls with phenolic foam, where the southwestern orientation showed considerably higher RH levels than northeast. The higher rain load from southwest caused only a slight increase in RH levels for the walls with insulating plaster compared with the northeastern orientation. Results indicate that the diffusion-open capillary active insulating plaster performs slightly better than the diffusion-tight phenolic foam when subjected to the large rain load and solar exposure from southwest. While to the northeast with its smaller rain load, the tight phenolic foam system performed better. This is in agreement with simulation results in [5, 10]. However, it should be noted that the water used for the installation of the insulating plaster may offset the tendencies as the systems may still dry out. Application of the exterior hydrophobisation had a positive effect on the performance of the phenolic foam oriented to the southwest, but not to the northeast.

Measurements for the wooden beam end (Fig. 5) showed increased RH levels for both the phenolic foam and insulating plaster compared with the un-insulated reference walls, but lower compared with the traditional mineral wool system. Despite the large difference in diffusion tightness between the phenolic foam and the insulating plaster, the two systems showed rather similar RH levels during the latter 10 months of the experimental period.

Comparison between orientations showed higher RH levels in the un-insulated reference wall and the insulated walls oriented to the southwest compared with northeast, due to the higher rain load. Exterior hydrophobisation had a positive effect on the performance of the two walls with phenolic foam, but the largest effect was seen for the wall to southwest.

In most test walls, the beam ends were seen to have lower RH levels than the wall plate, and thus smaller risk of moisture-induced problems. The lower RH levels were likely related to the beam end being in the centre of the thermal bridge created by the floor structure. Receiving a larger amount of heat from the indoor environment resulting in higher temperatures compared with the wall plate sensor that was fully covered behind the insulation. Moreover, the wall plate also had worse premises for redistribution of moisture to the indoor environment compared with the beam end, due to the position behind the insulation system and the direction of the pores in the wood. Wood have anisotropic properties with transport in the longitudinal direction, not in tangential direction.

The measurements showed that the effect of the hydrophobisation varied with the orientation for the

Table 2. Results from the on-site pH and mould growth tests, as well as VTT mould growth predictions for the interface (Point 3).

Wall ID \ Sample no.:	pH-value [-]		VTT mould index [-]		Mycometer value (MV)							
					Surface test in point 3 (interface):				Material test of drilling samples Outermost 10 mm of insulation[2]			
	Adhesive[1]	Lime render[1]	Point 3 Average	Point 3 Max	1a	1b	2a	2b	1a	1b	2a	2b
G1_MW_SW*		10	4.3	5.3	615	162			88	195	99	394
G3_Reference_SW		9.3										
G14_Reference_NE		9.2										
G5_Phenolic_SW	12.5	12.6	2.3	3.5	6	17	3	4	1	1	11	3
G6_Phenolic+H_SW	12.6	12.7	0.2	0.5	8	12	3	12	BDL	1	BDL	BDL
G11_Phenolic+H_NE	12.6	12.7	2.0	3.2	12	12	15	18	0	BDL	0	1
G12_Phenolic_NE	12.5	11.9	1.9	3.0	37	28	3	6	2	5	BDL	BDL
G8_Plaster_SW**	12.0	11.7	1.8	3.5	11	12	12	31	35	28	34	29
G9_Plaster+H_NE**	12.1	10.9	1.8	3.4	30	25	26	26	27	28	26	21

*Mycometer surface samples were taken on wooden studs, and material samples were taken at random from the mineral wool in the wall opening. **pH-value for insulating plaster as no adhesive was used for this system. BDL: below detection level. Sample "1" and "2" refer to the two drilling core samples taken out, while "a" and "b" refer to the two tests performed for each drilling core. [1]Average of two pH tests. [2]Samples from the outermost 10 mm of the insulation, near the interface between masonry and insulation.

phenolic foam insulation system. For the southwest oriented walls, the hydrophobisation highly reduced RH levels in the interface, wall plate and beam end as rain intrusion was an important factor. To the northeast however, a reduction due to the hydrophobisation was observed only for the beam end, while a slight increase was seen in both the interface and wall plate. This was possibly related to the differences between the two orientations with respect to wind driven rain and solar exposure. In Denmark, southwest oriented walls receive more rain and would thus benefit more from exterior hydrophobisation, and they are also subject to considerably more drying from solar radiation. The effect of hydrophobisation would be less on northeast oriented walls due to the smaller rain load, but at the same time, the walls would not have same drying potential due to less solar radiation. This was likely the reason why similar RH levels were seen for walls with and without hydrophobisation towards the northeast. In addition to the varying effect of orientation, the southwest oriented walls with phenolic foam also showed varying effect of hydrophobisation in the three different sensor locations. With a large reduction in RH levels occurring in the interface and wall plate, but a considerably smaller reduction in the beam end. Results suggests that this was likely related to the locations of the former two sensors being in or near the interface between wall and insulation where the risk of interstitial condensation was largest and where inwards moisture flow (summer condensation) would get stopped by the tight phenolic foam insulation, resulting in higher RH levels. In comparison, the beam end sensor was located in the centre of the thermal bridge of the floor beam, maintaining higher temperatures and lower RH levels. Any moisture from the outside would likely be transported to the indoor environment quite easily through the beam. Since rain intrusion was likely less important in the beam end due to these factors, the effect of the hydrophobisation was smaller.

The effect of hydrophobisation for the insulating plaster was difficult to evaluate as only the northeast oriented wall was treated. The intention was to create a worst case (untreated southwest) and best case scenario (treated northeast). However, results were found to be rather similar for both these walls in all three sensor locations, with only a slight reduction in the treated northeastern wall.

Note that the indoor moisture load of 60% RH was used throughout the experimental period, with the exception of January and February 2018 due to a malfunctioning humidifier. This was representative in a Danish context during summer periods, but abnormally high for winter periods. Danish best practice guidelines [4] suggest 30-50% RH during winter. A reduction would likely reduce the risk of moisture-induced problems as less moisture would be available in the indoor air for outwards diffusion.

3.2. pH and mould growth

Test of fresh material samples showed pH 12.7 for the lime render and the insulating plaster, and 12.4 for the adhesive mortar used for the phenolic foam insulation. The render and adhesive mortar in the test walls with phenolic foam maintained a high pH-value over the entire 2-year period (Table 2), and the adhesive mortar was even seen to increase slightly in pH compared with the fresh samples. The increase was likely due to the higher pH-value of the lime render affecting the adhesive mortar through washing out. Moreover, comparison between the four test walls fitted with phenolic foam showed little or no difference in the pH-value of the

render or adhesive mortar due to the exterior hydrophobisation. This corroborates with [15] who found no change in diffusion resistance of the masonry and mortar samples due to hydrophobisation treatment. Compared with the phenolic foam system, the insulating plaster and underlying render showed slightly lower pH-values. It should however be noted that the lime render on these walls were applied simultaneously with the render for the walls with phenolic foam, and was in direct contact with the room air for one year before application of the insulating plaster. This would likely have caused a decrease in pH-value for the render, and thus the render would not have had the same influence on the pH in the insulating plaster as it did for the adhesive mortar in the phenolic foam system. Moreover, the insulating plaster was highly diffusion-open while the phenolic foam system was diffusion-tight. This allowed for more rapid carbonation of the insulating plaster and the underlying render and reduction of the pH-values, compared with the phenolic foam system. The test wall with mineral wool and the reference walls experienced low pH-value, as rendered surfaces had direct contact with air over the 4½ years since application.

Table 3. Predicted mould growth using the VTT mould model for Point 5 (wall plate), and Point 6 (beam end).

Wall ID	Average VTT mould index [-]		Max VTT mould index [-]	
	P5	P6	P5	P6
G1_MW_SW	4.5	4.5	5.3	5.3
G3_Reference_SW	4.3	0.5	5.3	1.7
G14_Reference_NE	0.0	0.1	0.0	0.6
G5_Phenolic_SW	4.6	2.1	5.3	3.6
G6_Phenolic+H_SW	0.1	0.0	0.6	0.1
G11_Phenolic+H_NE	1.5	0.0	2.4	0.4
G12_Phenolic_NE	0.5	0.9	1.7	1.6
G8_Plaster_SW	2.6	1.1	5.2	2.7
G9_Plaster+H_NE	1.8	0.6	3.6	1.1

The on-site Mycometer surface and bulk material tests (Table 2) showed high mould growth for the traditional wall with mineral wool, vapour barrier and wood studs in the interface between wall and insulation, and above background level within the mineral wool layer. For the phenolic foam insulation and the insulating plaster, the tests showed mould growth within the normal background level (green marking) or slightly above background level (yellow marking, the smaller values). This indicates that the test walls with phenolic foam and insulating plaster did not experience mould growth within the first 1 or 2 years after application. This was despite the rather high RH levels observed in the interface between wall and insulation for some of the test walls, especially the walls without hydrophobisation. The lack of mould growth in these six test walls was likely due to the high pH-value in the material layers on both sides of the interface and little or no available nutrition resulting in unfavourable growth conditions. In contrast, the mould growth found in the test wall with mineral wool was most likely the result of high RH levels, available nutrition from the wood stud frame, and suitable pH-levels as samples were taking on the wooden studs and in the mineral wool.

The mould modelling results (Table 2 and 3) showed a large mould growth risk in both interface and embedded wooden elements for the test wall with mineral wool. For the reference walls, a potential risk was observed only for the wall plate in the southwest oriented test wall, while no risk was seen for the northeast oriented wall. Risk predictions for the walls with phenolic foam showed a medium to large risk of mould growth in the unhydrophobised southwest oriented wall. Meanwhile, the exterior hydrophobisation for wall G6 reduced the risk considerably, suggesting no mould growth in any of the three critical locations. Towards northeast, the effect of hydrophobisation was a bit mixed, showing reduced risk in the beam end, but increased risk in the interface and wall plate – as seen for the RH levels. For the insulation plaster, a slightly higher risk of mould growth was observed for the southwest oriented wall compared with the northeast oriented wall with hydrophobisation. For most test walls, the prediction indicate a higher risk in the wooden wall plate compared with the beam end. Note that the higher mould growth risk observed in the interface for the wall with mineral wool compared with the six other walls was due to the material sensitivity of the wooden studs being more sensitive compared with the insulating plaster and adhesive mortar, allowing for higher mould index values and at the same time a lower critical RH level.

Comparison between on-site Mycometer tests and the mathematical mould modelling were in agreement for the wall with mineral wool where both showed high mould growth risk, and for the southwest oriented wall with phenolic foam and exterior hydrophobisation where both methods showed no mould growth. However, contrasting results were seen for the remaining five walls, where the on-site testing found no mould growth in the interface between wall and insulation while the model suggests that all walls at some point during the period would reach a rather high mould growth risk with a final MI value of 3-3.5 within the 1 and 2 years of measurements. The reason for these discrepancies may relate to the lack of nutrition and the high pH-value of the adhesive mortar and insulating plaster hampering mould growth during the initial periods, as pointed out in [16]. pH-value was however not included in the mould model, and the duration of an “initial drying out” period was rather unclear. Morelli and Møller [9] found high pH-value in adhesive mortars 2 years after application. The reliability of some of the widely used mould prediction models were addressed in [17-18], who found that the models should not be used as a means to determine a precise risk of mould but rather to determine the likelihood of mould growth occurring or not. Alternatively, they could be used as comparative tools to assess different design solutions. Shortcomings within the models may relate to a lack of knowledge with

respect to mould growth on different materials and the effect of ageing of materials, as well as the definition of germination start and growth conditions, which were seen to differ between models. Due to the many unknown variables when dealing with mould growth in buildings, Gradeci et al. [19] proposed to use a probabilistic approach.

4 Conclusion

This paper presents a large field study comprised of several solid masonry walls with embedded wooden elements and internal insulation for up to two years. The hygrothermal performance of two insulation systems were assessed, and the risk of mould growth was determined through mathematical models and on-site testing. The effect of exterior hydrophobisation was also investigated.

The experiment showed that solid masonry walls retrofitted internally with phenolic foam and insulating plaster experienced high RH levels in one or more locations, when the exterior surfaces were left as bare brick and the indoor climate were kept at 60% RH throughout the year. Exterior hydrophobisation was shown to have a positive effect on the RH levels for walls insulated with phenolic foam. However, the effect of hydrophobisation was found to vary with the orientation and with the sensor locations. With limited or no reduction occurring for the northeast oriented wall with phenolic foam. With the given conditions, present findings suggest that exterior hydrophobisation is most crucial towards the prevailing wind direction, and are likely of be lesser importance on walls receiving a limited amount of wind driven rain.

No mould growth was found in the test walls with phenolic foam and insulating plaster, which was likely due to the combination of little to no available nutrition and high initial pH-value in the adhesive mortar and insulating plaster creating an unfavourable growth environment. This suggests that internal insulation could potentially be installed if proper cleaning prior to installation is done and the high pH-value is maintained. In contrast, mould growth was found in the test wall retrofitted with the traditional mineral wool and vapour barrier system, without high initial pH-value. A poor correlation was seen between the mathematical mould growth modelling and the on-site mould growth in the interface between wall and insulation. Post processing of the measured temperature and RH with the mould growth model overestimated the risk compared with the on-site tests. The observed discrepancies were likely due to the lack of available nutrition and the high pH-value in the interface hampering mould growth. However as mentioned earlier, the models could still serve as valuable tools to compare the hygrothermal performance of different design solutions. The authors recommend further validation of the prediction model through more experimental data. Perhaps in time including pH-value as a model factor.

This research was financially supported by the European Union's Horizon 2020 research and innovation programme under grant agreement No 637268 – as part of the RIBuild project; and by the Landowners Investment Foundation (Grundejernes Investeringsfond).

References

1. J. Kragh and K. B. Wittchen, Energy Build., vol. **68**, pp. 79–86 (2014)
2. T. Odgaard, S. P. Bjarløv, and C. Rode, Energy Build., vol. **162**, pp. 1–11 (2018)
3. J. Straube and C. Schumacher, J. Green Build., vol. **2**, no. 2, pp. 42–50 (2007)
4. E. Brandt, T. Bunch-Nielsen, G. Christensen, C. Gudum, M. H. Hansen, and E. B. Møller, *SBi-Anvisning 224 - Fugt i Bygninger 2nd ed. (Danish)* (2013)
5. E. Vereecken, L. Van Gelder, H. Janssen, and S. Roels, Energy Build., vol. **89**, pp. 231–244 (2015)
6. H. Viitanen, J. Vinha, K. Salminen, T. Ojanen, and R. Peuhkuri, J. Build. Phys., vol. **33**, pp. 201–224 (2010)
7. P. Klõšeiko, E. Arumägi, and T. Kalamees, J. Build. Phys., vol. **38**, no. 5, pp. 444–464 (2015)
8. T. Odgaard, S. P. Bjarløv, and C. Rode, Build. Environ., vol. **129**, pp. 1–14 (2018)
9. M. Morelli and E. B. Møller, Sci Technol Built En, vol. **25**, no. 9, pp. 1199–1211 (2019)
10. E. Vereecken and S. Roels, Energy Build., vol. **80**, pp. 37–44 (2014)
11. T. De Mets, A. Tilmans, and X. Loncour, Energy Procedia, vol. **132**, pp. 753–758 (2017)
12. Diasen, *Diathonite Thermactive.037*, [Online]. https://www.diasen.com/sp/en/p/diathonite-thermactive-037.3sp, Accessed: 07.06.2018
13. T. Ojanen, H. Viitanen, R. Peuhkuri, K. Lähdesmäki, J. Vinha, and K. Salminen, *Thermal Performance of the Exterior Envelopes of Whole Buildings - 11th International Conference*, (2010)
14. M. Reeslev and M. Miller, Proc. Heal. Build., vol. **1**, pp. 589–590 (2000)
15. T. K. Hansen, S. P. Barløv, R. H. Peuhkuri, and K. K. Hansen, Constr. Build. Mater., vol. **188**, pp. 695-708 (2018)
16. H. Viitanen, M. Krus, T. Ojanen, V. Eitner, and D. Zirkelbach, Energy Procedia, vol. **78**, pp. 1425-1430 (2015)
17. K. Gradeci, N. Labonnote, B. Time, and J. Köhler, Constr. Build. Mater., vol. **150**, pp. 77–88 (2017)
18. E. Vereecken and K. Vanoirbeek, J. Build. Phys., vol. **39**, no. 2, pp. 102–123 (2015)
19. K. Gradeci, U. Berardi, B. Time, J. Köhler, Energy Build., vol. **177**, pp. 112-124 (2018)